FACTORS, ORIGIN AND SOURCES AFFECTING PM1 CONCENTRATIONS AND COMPOSITION AT AN URBAN BACKGROUND SITE

Squizzato, S., Masiol, M., Agostini, C., Visin, F., Formenton, G., Harrison, R. M., & Rampazzo, G.

Published in Atmospheric Research, 180, pp. 262-273

DOI: https://doi.org/10.1016/j.atmosres.2016.06.002

FACTORS, ORIGIN AND SOURCES AFFECTING PM_1 CONCENTRATIONS AND COMPOSITION AT AN URBAN BACKGROUND SITE

Stefania Squizzato[*,1], Mauro Masiol[2,3], Chiara Agostini[1], Flavia Visin[1], Gianni Formenton[4], Roy M. Harrison[2,†], Giancarlo Rampazzo[1]

[1]Dipartimento di Scienze Ambientali, Informatica e Statistica, Università Ca' Foscari Venezia, Campus scientifico, Via Torino 155, 30172 Mestre (VE), Italy
[2]Division of Environmental Health and Risk Management School of Geography, Earth and Environmental Sciences University of Birmingham Edgbaston, Birmingham B15 2TT United Kingdom
[3] Center for Air Resources Engineering and Science, Clarkson University, Box 5708, Potsdam, New York 13699, USA
[4]Dipartimento Regionale Laboratori, Agenzia Regionale per la Prevenzione e Protezione Ambientale del Veneto (ARPAV), Via Lissa 6, 30174 Mestre (VE), Italy

ABSTRACT

[*] To whom correspondence should be addressed.
Tele: +39 041 234 8639, Email: stefania.squizzato@unive.it; stefania.squizzato81@gmail.com

[†]Also at: Department of Environmental Sciences / Center of Excellence in Environmental Studies, King Abdulaziz University, PO Box 80203, Jeddah, 21589, Saudi Arabia

PM_1 is widely believed to provide better information on the anthropogenic fraction of particulate matter pollution than $PM_{2.5}$. However, data on PM_1 are still limited in Europe as well as comprehensive information about its chemical composition and source apportionment and this gap is more evident in the pollution hot-spots still remaining in Europe, such as the Po Valley (Northern Italy). Elemental and organic carbon, 7 water soluble inorganic ions and 17 elements were quantified in 117 PM_1 samples collected at an urban background site in Venice-Mestre, a large city located in the eastern Po Valley, during winter (December 2013 – February 2014) and summer (May-July 2014) periods.

Results show a strong seasonality for PM_1 mass concentration (averages ranging from 6±2 in summer to 34±24 μg m^{-3} in winter) and for most of the analyzed species. Components mainly related to road traffic, residential heating, biomass burning and secondary inorganic aerosol (ammonium nitrate) reached their highest levels in winter, while mineral dust and marine components were elevated in summer. PMF analysis revealed 7 potential sources. Secondary inorganic aerosol (33%) and biomass burning (33%) are the major contributor in winter followed by EC-primary emissions (16%), aged sulphate (6%), road traffic (7%), fossil fuel combustion (%) and marine aerosol (3%). During summer, these sources account for 12%, 14%, 20%, 22%, 8%, 14% and 10%, respectively.

Some PM_1 sources are located near the sampling site (residential area, traffic road, industrial area) but a major contribution of long range transport is observed when high pollution events occur. The results give useful insights into PM_1 composition in an urban area and chemical profiles of sources helpful in the interpretation of receptor model results.

Keywords: PM_1, water soluble inorganic ions, carbonaceous materials, mass closure, PMF

1. INTRODUCTION

In recent decades, the characterisation of airborne particulate matter (PM) has become an increasingly important topic of research since the epidemiological data have showed that PM has negative effects upon human health (Anderson et al., 2012; Rohr and Wyzga, 2012). Fine particles (with aerodynamic diameters of less than 2.5 μm, $PM_{2.5}$, and 1 μm, PM_1) may play an important role in affecting human health for a number of reasons: (i) they penetrate more effectively into the deep lung; (ii) they can penetrate more readily into indoor environments; (iii) they can remain suspended for longer periods of time in the atmosphere than coarse particles; (iv) they may be transported over long distances; (v) they tend to carry higher concentrations of the more toxic compounds, including acids, heavy metals and organic compounds and (vi) they have a larger surface area per unit mass compared to larger particles and, thus, can absorb larger amounts of semi-volatile compounds (e.g., Pope and Dockery, 2006). Consequently, the study of levels, composition and emission sources of fine particles in densely populated areas is very important for health protection and to improve PM control strategies.

Fine particles are typically mainly composed of elemental carbon (EC), organic carbon (OC), inorganic ions and metals. Among these major components, some studies have associated carbonaceous particles with health effects (Rohr and Wyzga 2012). These consist of compounds from combustion exhaust, soil, paved road dust, cooking and other sources (Harrison and Yin, 2008). EC comprises small (mainly sub-micrometre) graphitic particles which arise from primary emissions from combustion of various fuels, e.g., coal, wood, fuel oil and motor fuel, especially diesel. Organic carbon (OC) can be directly emitted into the atmosphere in the particulate phase or can originate in the atmosphere from gas-to-particle conversion processes (forming the so-called secondary organic aerosol, SOA) (Seinfeld and Pandis, 2006). Generally, EC lies in the submicrometre range, whereas OC exhibits wider size distributions (Pio et al., 2007).

Inorganic ions can be emitted from various primary sources, such as combustion, sea salt and crustal material. However, the main source of sulphate, nitrate and ammonium is the generation of

secondary inorganic aerosol (SIA) through (photo-) chemical reactions of gaseous precursors (NO_x, SO_2, NH_3) and O_3 with atmospheric oxidants to form mainly ammonium nitrate (NH_4NO_3) and ammonium sulphate ($(NH_4)_2SO_4$)) (Seinfeld and Pandis, 2006).

Although metals generally represent a small fraction of PM_1 mass, their contribution to the overall toxicity of particles cannot be disregarded. The chemical and physical properties of some elemental species is size-dependent: for example, the solubility of Pb, Co and Cd increase in fine particles, making those elements more bioavailable (Birmili et al., 2006). The characterisation of elemental composition is also very important for source apportionment studies: the variable proportion of some well known elemental markers can help in the identification of potential sources using receptor modelling techniques.

Although it has been suggested that PM_1 can provide a better estimation of anthropogenic particles than $PM_{2.5}$ (Perrone et al., 2013), PM_1 source apportionment studies are still limited in Europe as well as comprehensive information about its composition (e.g. Perez et al., 2008; Vecchi et al., 2008; Theodosi et al., 2011; Perrone et al., 2013). Moreover, PM_1 is not yet regulated in Europe and this is a major reason why there is a lack of available data and studies upon it. This is a serious gap, as some air pollution hotspots still remain in highly populated areas of Europe. Among others, the Po Valley (Northern Italy) deserves particular attention because of the frequent exceedance of guidelines and Limit Values fixed by EC Directives and international organizations such as WHO (Larsen et al., 2012). The present paper aims to investigate the composition of PM_1 in Mestre-Venice, a large city on the eastern border of the Po Valley. Here, the highest concentrations of particulate matter and nitrogen oxides ($NO+NO_2=NO_x$) are commonly recorded in winter, while high levels of ozone are measured in summer due to photochemical processes involving precursors of natural and anthropogenic origin (Masiol et al., 2014a;b).

106 PM_1-bound elemental and organic carbon, water soluble inorganic ions and elements, have been
107 analysed to determine the major contributors to PM_1 mass and were then processed to (i) determine
108 the seasonal cycles, (ii) estimate secondary inorganic and organic aerosol, (iii) assess the major
109 components applying a mass closure model, (iv) identify and quantify the most probable sources by
110 using a receptor modelling technique (positive matrix factorization, PMF) and (v) hypothesize their
111 location applying a conditional probability function.
112
113 **2. MATERIAL AND METHODS**
114 **2.1 Measurement Site**
115 Venice is located between the eastern edge of the Po Valley and the Adriatic Sea. Along with the
116 city of Mestre, they form a large coastal urban municipality hosting 270,000 inhabitants (~ 628
117 inhabitants km^{-2}) (ISTAT, 2011). The local emission scenario includes some major potential
118 sources of PM: high density residential areas; heavily trafficked roads mostly congested during
119 peak hours; a motorway and a motorway-link which are part of the main European routes E55 and
120 E70; an extended industrial area (Porto Marghera) and an international airport.
121
122 The sampling site (Via Lissa-Mestre, Lat. 45.4871 N –Long. 12.2229 E) is located in a highly
123 populated residential zone of Mestre surrounded by several heavily trafficked roads (distance ~ 450
124 m) (Fig. 1). The site was categorized as urban background by the local environmental agency
125 (ARPAV). It lies about 200 m from an important motorway and few meters from the railway.
126 Moreover, Via Lissa was chosen considering the background of information on $PM_{2.5}$ composition
127 (Masiol et al., 2014b) that can help in the interpretation of PM_1 data.
128
129 **2.2 Experimental**
130 PM_1 samples were collected daily (117 samples) at an urban background site in Venice (Via Lissa-
131 Mestre) during winter (December 2013 – February 2014) and summer (May-July 2014) periods

using a low volume sampler (Skypost PM, Tecora, Milan) on quartz fiber filters. Sampling time was 24 h, from 0:00 to 24:00 and the flow rate was 2.3 $m^3 h^{-1}$. PM_1 masses were measured by gravimetric determination (microbalance with 0.1 µg sensitivity) on filters preconditioned for 48 h at constant temperature (20°C) and relative humidity (50%).

Half of each sample was digested for elemental determination. Acid digestion was performed using 4 mL of 69% HNO_3, 1 mL H_2O_2 and 0.3 mL 48.9% HF in a microwave oven using the protocol proposed by Karthikeyan et al. (2006). An ICP-OES (Optima 5300 DV, Perkin Elmer) was used to determine the mass concentration of Mg, Al, S, K, Ca, Ti, Mn, Fe, Zn, Ba while an ICP-MS (Elan 6100, Perkin–Elmer) was used for V, Ni, Cu, As, Cd, Sb, Pb.

For the analysis of ion components an aliquot (16 mm Ø disc) was punched from the filter. Punches were extracted in vials with 10 mL MilliQ water (resistivity= 18.2 MΩ•cm at 25°C, Millipore) and sonicated for 50 min. Extracts were pre-filtered on microporous (0.45 µm) PTFE membranes and injected in two Metrohm (Switzerland) ion chromatographic systems with conductivity detectors to quantify the concentrations of three anions (Cl^-, NO_3^-, SO_4^{2-}) and five cations (Na^+, NH_4^+, K^+, Mg^{2+}, Ca^{2+}). The analytical ion chromatography method is reported elsewhere (Masiol et al., 2015a). Finally, an aliquot of filter (1 cm^2) was analysed for elemental and organic carbon by using a Thermal–Optical Carbon Aerosol Analyser (Sunset Laboratory, Forest Grove, OR, USA) following the EUSAAR2 protocol (Table SI1). The carbon analyzer employs a programme of temperature and gas composition to evolve carbon species and a laser at a wavelength of 680 nm to monitor the filter transmittance (Birch and Cary, 1996).

Field blanks were prepared and analyzed together with the samples and the values obtained were routinely subtracted. Limits of detection (LODs) were calculated as three times the standard

deviation of field blanks (Table SI2): data below the LODs were substituted by LOD/2 for the statistical processing.

Gaseous pollutants data were provided by ARPAV (local environmental protection agency for Veneto region) whereas meteorological data refer to station 5 of the monitoring network of Ente Della Zona Industriale di Porto Marghera.

2.3 QA/QC and Uncertainties

The quality of the analytical procedures was checked by blank controls, by evaluating detection limits (DLs), recoveries, accuracy, and repeatability. The accuracies of quantitative analyses were assessed by analyzing certified liquid standards (TraceCERT, Fluka) for standard reference materials for elements (SRM 1648, NIST). OC and EC analyses were routinely checked by re-analysing sucrose calibration standards (relative standard deviation <4%). The recoveries of ions and elements were in the range of 80–110%. The relative standard deviation of each ion and elemental recoveries was < 5%.

2.4 PMF Settings

USEPA PMF 5.0 was used in this study. PMF was performed strictly following the main rules and suggestions found in the user manual (USEPA, 2014) and in Reff et al. (2007). Details of PMF settings and regression diagnostics are provided as supplementary materials (SI1 and Table SI3).

Data and uncertainties were handled according to Polissar et al. (1998): (1) data < DLs were set as DL/2, with an uncertainty of 5/6 of the corresponding DL; (2) data > DLs were matched with uncertainties determined by compounding errors from the most uncertain components with the addition of 1/3 of the DLs.

183 # 3. RESULTS AND DISCUSSION

184 ## 3.1 Overview on PM_1 Levels and Composition

185 ### 3.1.1 PM levels and main components

186 Table 1 summarizes the average seasonal concentrations of PM_1 and its components, gaseous
187 pollutants and meteorological variables. The average PM_1 concentration over the whole period was
188 21±22 µg m^{-3}. PM1 concentrations show the typical pattern of the study area, lower in warmer
189 seasons and higher in the colder period (6.4±2.2 µg m^{-3} and 34±24 µg m^{-3} mean, respectively).
190
191 Measured levels are comparable with those observed by Perez et al. (2008) (19 µg m^{-3} annual mean)
192 at an urban background site in Barcelona (Spain) (5.8 µg m^{-3}, summer time) and with those
193 previously detected in Venice by Valotto et al. (2014) (26.6 µg m^{-3}, winter time). Moreover, similar
194 concentrations during winter were observed at other sites in Italy whereas summer concentrations in
195 this study tend to be lower (Vecchi et al., 2004; Vecchi et al., 2008) but comparable with those
196 observed in Birmingham (UK) (Harrison and Yin, 2008) (Table 2). This may be due to the higher
197 wind speeds experienced in the summer period that tend to favour PM dispersion resulting in a drop
198 of concentration. Furthermore in the study area PM_1 is strongly associated with mixed combustion
199 processes dominating in winter including domestic heating (Valotto et al., 2014).
200
201 During winter the PM_1 fraction makes a major contribution to PM_{10}, averaging about 60% of PM_{10}
202 mass. On the contrary, the coarse fraction prevails in summer when the PM_1 contribution to PM_{10}
203 tends to be lower (40% on average). Similarly, PM_1 represents about 60% of $PM_{2.5}$ with the highest
204 percentage in winter and the lowest in summer (67 and 43% of mean, respectively) (Table 2).
205
206 Chemical composition measurements of PM_1 showed that total carbon (TC) and secondary
207 inorganic aerosol (SIA) represent the main components reaching 34% and 22% of the annual mean,
208 respectively. During winter these components make up about 68% of PM_1, on the contrary during

209 the summer the elemental contribution increases and reaches 24%, whereas TC and SIA contribute
210 25% and 18% of PM_1 mass, respectively.
211
212 **3.1.2 Water soluble inorganic ions**
213 Ammonium, nitrate and sulphate contribute about 76 % of the total inorganic ionic species mass
214 (83% and 69% in winter and summer periods, respectively). As previously observed in $PM_{2.5}$
215 samples (Squizzato et al., 2013), sulphate dominates over nitrate in summer whereas in winter
216 nitrate dominates over sulphate. This behaviour can be explained by the semi-volatility of
217 ammonium nitrate. Other anions and cations contribute a minor fraction of the water-soluble
218 species (17 and 31% in winter and summer, respectively). All concentrations of Ca^{++} were below
219 the detection limit.
220
221 Ammonium and sulphate are correlated both in the winter and summer periods (r=0.79 and r=0.78,
222 respectively). Nitrate, whose concentrations strongly depend on the meteorological conditions,
223 shows a strong correlation with both ammonium and sulphate during winter (r=0.97 and r=0.75,
224 respectively), but during summer the correlation with ammonium is lower (r=0.53) and practically
225 absent with sulphate (r=0.24).
226
227 As proposed by Cheng et al. (2011), a comparison between the calculated and observed NH_4^+
228 concentrations was conducted to evaluate the formation of secondary ions (Figure 2). The NH_4^+
229 concentration can be calculated based on the stoichiometric ratios of the major compounds (i.e.
230 ammonium sulphate [$(NH_4)_2SO_4$], ammonium bisulphate [NH_4HSO_4] and ammonium nitrate
231 [NH_4NO_3]); assuming that NO_3^- is in the form of NH_4NO_3 and that SO_4^{2-} is in the form of either
232 $(NH_4)_2SO_4$ or NH_4HSO_4. During winter, the slope is 0.98 when $(NH_4)_2SO_4$ is assumed and 0.88
233 when NH_4HSO_4 is assumed. This suggests that aerosol is fully neutralized by available ammonia.
234 Summer samples present different relationships: the slope was 2.86 and 1.70 assuming $(NH_4)_2SO_4$

235 and NH_4HSO_4, respectively. In this case, the aerosol may be acidic (i.e., not fully neutralized with
236 available NH_4^+) and mainly in the form of NH_4HSO_4. However, the pronounced scatter in the
237 summer data in Figure 2 suggests that other forms of sulphates and nitrates may be present. Despite
238 this, the anion/cation balance shows neutral conditions (Figure SI1) and no significant differences
239 can be observed between winter and summer with slopes of 0.90 (r^2=0.98) and 0.93 (r^2=0.80),
240 respectively.
241
242 Ammonium nitrate is a semi-volatile species and exists in reversible phase equilibrium with nitric
243 acid in the gas phase. At higher temperatures and lower relative humidity, ammonium nitrate will
244 evaporate. At temperatures exceeding 25°C (as in our summer conditions) evaporation is almost
245 complete (Schaap et al., 2004) and this can lead to a deficiency of ammonium in the summer
246 samples. The volatilised nitrate, in the form of nitric acid, can react with other cations. Na^+ is the
247 second most abundant cation presents in PM_1 samples; hence the relationship between sodium,
248 nitrate and chloride (considering NaCl as the main form of sodium in the study area due to the
249 proximity of the sea) was investigated by using a multiple regression analysis. During winter, Na^+ is
250 mainly present in the form of NaCl (Na^+= 0.31 +1.03[Cl^-] - 0.47[NO_3^-]; r^2_{adj}=0.68), while during
251 summer Na^+ can also be present as $NaNO_3$ (Na^+= 0.93[Cl^-] +0.15[NO_3^-]; r^2_{adj}=0.94), maintaining
252 the neutral conditions previously observed.

253 **3.1.3 Elements**

254 On an annual basis nitrate, sulphate, ammonium, potassium and calcium represent the main
255 inorganic components of PM_1. The Kruskal-Wallis test was applied to evaluate intra-seasonal
256 differences. Among the analysed elements only Ti, Ba, Ni, Cd and Sb do not show a statistically
257 significant seasonal difference ($p>0.05$). The others present a marked seasonal difference, with the
258 higher concentration in winter, except for Ni and V.
259

Ni and V show the highest mean concentration during summer. This behaviour has been observed in a previous study (Masiol et al. (2014b); fossil fuel emissions (identified by Ni-V association) reached their highest levels in spring and summer in $PM_{2.5}$ and showed a significant drop in winter. These elements are strongly associated with combustion of fuel oil, and increased shipping traffic in the cruise harbour.

Sulphur is present mainly as sulphate in both the winter and summer period, and shows a higher average concentration in winter. Potassium is mainly present in the ionic form probably linked to wood combustion for residential heating (McDonald et al., 2000). Scatterplots between element and ionic form are provided as supplementary material (Figure SI2). Considering the uncertainties associated with low concentrations, LODs and concentration of total Ca and soluble Ca (Ca^{++}), it could be stated that almost all calcium is in insoluble form.

Average elemental concentrations have been computed for working days (from Monday to Friday) and week-end days (Saturday, Sunday and holidays) to highlight which elements are mainly associated with working cycles. The largest differences were observed in winter. Among the determined elements, Mn and Ni increase strongly during working days (Mn +105%; Ni +65%) and Ca, Mg, Zn and V show a slight enrichment (+27%, +15%, +26% and +22%, respectively). These elements are associated with road traffic emissions due to tyre wear, brake wear and resuspension (Pant and Harrison, 2013 and references therein). Moreover all these elements are often present predominantly in the finer fraction (<0.61 μm) and in intermediate fractions (0.61 -4.9 and 1 - 4 μm) (Fernandez Espinosa et al., 2001; Masiol et al., 2015b; Samara and Voutsa, 2005).

Compositional data have been compared with those observed at the same site for a previous $PM_{2.5}$ campaign (Masiol et al., 2014b) (Table 2). NO_3^-, Mn, Cu, V, Ni, As and Cd appear to be enriched in the finest fraction whereas Ti, Fe, S and Pb are mainly distributed in the $PM_{1\text{-}2.5}$ fraction. Table 2

286 also reports a comparison of PM elemental composition with other studies. Generally, higher
287 concentrations have been observed for Ca, Mg, Al in our study. Other elements present comparable
288 concentrations or are slightly lower than other studies.
289
290 **3.1.4 Carbonaceous aerosol**
291 Over the whole period OC ranged from 0.4 to 45.0 µg m^{-3} and EC ranged from 0.1 to 9.6 µg m^{-3}.
292 Both components show a marked seasonal pattern with the higher concentrations in winter and the
293 lower in summer (Table 1). As EC is a primary pollutant, derived from ground-level combustion
294 processes, this behaviour is expected due to less effective dispersion processes in the cold period.
295 Measured concentrations are of the same order of those observed in other Italian cities and lower
296 than those detected in Barcelona (Spain) and Birmingham (United Kingdom) (Table 2).
297
298 During winter EC is strongly correlated with carbon monoxide (r=0.89) and NO_x (r=0.85), and
299 similarly OC shows a strong correlation with carbon monoxide (r=0.93) and NO_x (r=0.86). On the
300 other hand, during summer both components present weaker correlations with CO and NO_x
301 (r_{EC_CO}=0.61, r_{OC_CO}=0.49; r_{EC_NOx}=0.53, r_{OC_NOx}=0.39). It is not clear if CO and NO_x are mainly
302 associated with traffic or with domestic heating emissions in the study area. Considering the
303 recently released emissions inventory (ISPRA, 2015), CO emissions are mainly due to non-
304 industrial combustion plant (39% and the greatest part linked to emissions from residential plant),
305 road transport (36%) and other mobile sources (21%). As regards NO_x emissions, 40% was
306 attributed to road transport, 27% to other mobile sources and only 7% to non-industrial combustion
307 plant. However, weak correlation of both EC and OC with primary gaseous pollutants during the
308 summer period suggests that combustion processes for domestic heating could be the principal
309 source of EC and primary OC in winter and the secondary organic component may dominate in
310 summer.
311

In the literature, the ratio between organic carbon and elemental carbon may be a first indication of the nature of the aerosol, namely if they are primary (POC) or secondary (SOC) organic carbon. Ratios greater than 2.0 - 2.5 may indicate the presence of secondary, therefore "aged" aerosols (Turpin and Huntzinger, 1995; Bougiatiati et al., 2013). Organic carbon concentrations are expected to be higher in such aerosols because of secondary aerosol formation via condensation of lower-volatility organic compounds onto particles as a result of photochemical reactions and oxidation rendering the organic species less volatile and enabling their partition to the particulate phase (Donahue et al., 2006). On this basis, SOC concentrations might be expected to be higher in summer than in winter period arising from enhanced photochemical formation (Harrison and Yin, 2008), but the lower temperatures in winter favour partitioning into the condensed phase.

To better understand the relative amounts of POC and SOC, the EC-tracer method proposed by Castro et al. (1999) as used by Harrison and Yin (2008) have been applied to winter and summer data, separately to limit the influence of atmospheric conditions. In the EC-tracer method, EC is used as a tracer for POC. These methodologies aim to determine the primary OC-EC ratio by identifying the periods where ambient concentrations are dominated by primary emissions, with SOA simply appearing as an increase in the OC/EC ratio relative to that of the primary OC/EC ratio (Turpin and Huntzinger, 1991).

The approach proposed by Cabada et al. (2004) consists of three main steps, briefly: (i) removal from the original dataset of the points where rain causes significant changes to the OC/EC ratio; (ii) identify days characterised by high probability of SOA formation by using ozone concentrations, in this study SIA has been used as indicator of secondary formation processes and days with both a high SIA concentration and high OC/EC ratio have been removed; (iii) identify periods where combustion-related sources dominated by using CO concentration; days when the OC/EC ratio drops in correspondence with high CO concentration are used to estimate the primary OC/EC ratio.

Harrison and Yin (2008) propose to plot OC concentration as a function of EC, then the lower bound of the data points is generally taken to represent a constant mixture of EC with primary OC. Points lying above that minimum ratio line contain additional OC, which is interpreted as being secondary.

Assuming that OC primary can be defined by,

$$[POC] = [OC/EC]_p * [EC] + b,$$

the contribution of secondary OC can be estimated as

$$[SOC] = [OC] - [POC],$$

Where [POC] is the primary organic aerosol concentration, $[OC/EC]_p$ is the ratio of OC to EC for the primary sources affecting the site of interest, and *b* is the non-combustion contribution to the primary OC and sampling artefact (Cabada et al., 2004 and references therein). In the method proposed by Harrison and Yin (2008) *b* has been set to zero.

Despite the OC/EC ratio presenting higher values during winter than in summer (3.1 and 1.6 means, respectively) indicating a greater contribution of secondary aerosol during the winter, the percentage contribution of SOC to total OC is higher in summer (54%) than in winter (39.5%) for both methods used (Table 3). This is in agreement with the enhanced photochemical formation due to the increase of solar radiation during summer.

In order to gain further insights, POC was compared with K^+ concentrations, considering soluble potassium as a marker of biomass burning and thus of primary emission from this combustion source. Similarly, SOC was compared with NO_3^- and SO_4^{2-} representing the secondary inorganic aerosol. During winter K^+ shows high correlations with calculated POC and SOC. On the other hand, during summer when wood combustion is less prevalent and the secondary inorganic aerosol formation is less favoured with respect to winter, the correlation is lower between K^+ and POC and absent between SOC, NO_3^- and SO_4^{2-} (Table 3).

3.2 Mass closure for PM_1

A mass closure model has been constructed by using previously developed conversion factors for $PM_{2.5}$. The conversion factors adopted are reported in Table 4. As such, PM reconstructed mass (RM) equation takes the following form:

RM = Secondary inorganic ions + OM (Organic Matter) + EC + Mineral dust + Salts + Heavy elements + K^+

On the basis of previous observed relationships, some specific conversion factors have been applied to summer data: sulphate has been considered as NH_4HSO_4 and nitrate has been assumed as NH_4NO_3 and $NaNO_3$ according to the relation $Na^+ = 0.93[Cl^-] + 0.15[NO_3^-]$.

Although the selected conversion factors have been usually applied to PM_{10} and $PM_{2.5}$ data (Harrison et al., 2003; Chow et al., 2015), good results were obtained. A good model fit is demonstrated by three factors: high r^2, gradient close to 1.0 and a near-zero intercept (Yin and Harrison, 2008). According to these criteria, a very good mass closure fit was found in winter: high r^2 (0.96), gradient close to 1 (0.96) and near-zero intercept (0.17 $\mu g\ m^{-3}$). In summer, the mass closure fit can be considered good (r^2 = 0.65, gradient 1.39 and intercept -1.27 $\mu g\ m^{-3}$) indicating a

389 lower reconstructed mass than that measured. Results are consistent with those observed by Yin and
390 Harrison (2008) on PM_1 samples. Regression equations are reported in Table 4 and the average
391 composition of winter and summer samples appears in Fig. 3.
392
393 During winter OM and secondary components dominate the PM mass. On the other hand, in
394 summer the major contributor to PM is mineral dust and the marine component (NaCl) increases
395 linked to the sea-land wind regime that enhances the movement of air masses from the sea to the
396 land during the daytime. When high pollution events occur (PM_1>50 µg m^{-3}, 17 days) no significant
397 differences were observed in PM_1 composition, including a simultaneous increase of all
398 components. Meteorological conditions can partially explain the enhanced concentration: a
399 relatively lower temperature (7°C) and wind speed (1 m s^{-1}) with respect to the mean of the winter
400 favour the condensation of secondary compounds and the accumulation of PM components.
401 Furthermore, as observed for $PM_{2.5}$ samples (Squizzato et al., 2012), long range transport should
402 contribute to the increase of PM concentrations.
403
404 **3.3 PM_1 Sources**
405 Seven factors were extracted from the PMF model. Modelled PM_1 mass concentrations successfully
406 predicted PM_1 (r^2 = 0.97) and all scaled residuals were normally distributed.
407 The source profiles obtained are given in Fig. 4 while time series and apportioned mass
408 contributions on a seasonal basis are given in Fig. SI3. Results were interpreted on the basis of the
409 presence of known tracers for the specific sources and considering seasonal variations:
410 • EC characterises the first extracted factor: this factor can represent the primary contribution to
411 PM_1 considering EC as a marker of primary emissions from combustion processes
412 (combustion of coal, fuel oil and motor fuel, especially diesel). Seasonally it contributes 6 and
413 2 µg m^{-3} (16% and 20%) of PM_1 concentrations in winter and summer, respectively. Despite

414 the marked meteorological difference between winter and summer, the primary contribution
415 appears to represent a rather invariant percentage of total mass.
416 • The second factor accounts for a large proportion of K^+ and OC: this association well
417 describes the biomass burning combustion source (Reche et al., 2012). The high percentage
418 contribution to PM_1 reached in winter (33%) confirms this hypothesis. The close relationship
419 between K^+ and OC has been already been discussed in the previous section.
420 • Fe, Mn, Zn, Ni, Cu and Sb are the main markers of the third factor: they represent a mix of
421 elements related to traffic as non-exhaust particle emissions. It has been shown that even with
422 zero tail pipe emissions, traffic will continue to contribute to fine particles through non-
423 exhaust emissions and it is estimated that nearly 90% of the total emissions from road traffic
424 will come from non-exhaust sources by the end of the decade. These elements arise from tyre
425 wear, brake wear and resuspension (Pant and Harrison, 2013 and references therein). As with
426 the EC primary emission, this source does not show a seasonal difference, contributing 7%
427 and 9% of PM_1 in winter and summer, respectively.
428 • The fourth factor explains more of 80% of vanadium concentration and 40% of cadmium: this
429 association can represent a mixed contribution of fossil fuel combustion, petrochemical plant
430 (V) and industrial activities such as steel production and zinc metallurgy (Cd) (Querol et al.,
431 2007) probably related to the proximity (about 6 km) of the industrial area of Porto Marghera.
432 Usually, V-Ni is the typical pair of elements indicative of fuel oil combustion, however
433 Moreno et al. (2007) observed that this relationship is stronger in the coarse particles than in
434 the fine particles. In this case, PMF is not able to split this factor into two different sources.
435 This factor contributes to 3% and 14% of PM_1 in winter and summer, respectively.
436 • The marine component is highlighted in the fifth factor (Na^+, Cl^- and Mg): despite sea-salt
437 particles being mainly distributed in the coarse fraction, some particles, are also present in the
438 fine fraction. Marine contributions increase during summer (10%, 1 $\mu g\ m^{-3}$) due to the sea-
439 land breeze wind regime.

- In the sixth factor, sulphate and Mg are associated: this factor is interpreted as aged sulphate due to the ageing of sea-salt aerosols i.e. to heterogeneous reactions with atmospheric S(VI), from the oxidation of S(IV) species. Similar to the previous factor, the highest contribution can be observed in summer (22%, 2 μg m^{-3}) due to the advection of air masses from the Adriatic Sea and the Venice Lagoon.
- The last factor represents the secondary inorganic component of PM_1: it links NH_4^+, NO_3^- and SO_4^{2-} to a lesser extent. These secondary ions derive from gas-to-particle conversion processes involving (photo-) chemical reactions of gaseous precursors such as NO_x, SO_2 and NH_3. The highest contribution is reached in winter (33%, 12 μg m^{-3}) when the meteorological conditions (low temperature and high relative humidity) and the higher concentration of NO_x tend to favour the formation and stability of ammonium nitrate.

In order to evaluate the possible location of each identified source and to confirm PMF results, CPF (conditional probability function) analysis has been applied to PMF source contributions. To minimize the effect of atmospheric dilution and seasonal behaviour, the daily fractional contributions from each source relative to the total of all sources were used rather than the absolute source contributions (Kim et al., 2003). The CPF estimates the probability that a given source contribution from a given wind direction will exceed a predetermined threshold criterion. CPF is defined as:

$$CPF = \frac{m_{\Delta\theta}}{n_{\Delta\theta}}$$

where $m_{\Delta\theta}$ is the number of occurrences from wind sector Δθ (11.25 degree) that exceeded the threshold criterion, and $n_{\Delta\theta}$ is the total number of data from the same wind sector. Calm winds (< 1 m s^{-1}) were excluded from this analysis due to the isotropic behaviour of the wind vane under calm winds. The threshold criterion has been fixed to the upper 25th percentile of the fractional

464 contribution of each source. The sources are likely to be located in the directions that have high
465 conditional probability values (Kim et al., 2005).
466
467 CPF values for each source that apportion to PM_1 are plotted in polar coordinates in Fig. 5. Lowest
468 directional probabilities are seen for biomass burning and secondary inorganic aerosol sources: this
469 should reflect a widespread pollution over the study area. Other sources show specific directions
470 associated with the highest probabilities. The highest probabilities for primary aerosol are reached
471 towards the north probably due to vehicle emission from the motorway link and urban traffic.
472
473 Road traffic shows high probabilities towards the north-west and south-east in correspondence with
474 a heavy trafficked road and railway close to the sampling site confirming that this source is mainly
475 associated with the resuspension of road dust rather than exhaust emissions.
476
477 Marine aerosol and aged sulphate show similar patterns with the highest probabilities towards the
478 south-east in correspondence with the Venice Lagoon and the Adriatic Sea about 5 km and 15 km
479 distant, respectively, supporting PMF source interpretation.
480
481 The high probabilities associated with fossil fuel combustion occur for wind blowing from the south
482 where the industrial area of Porto Marghera is located, confirming that this source should be related
483 to industrial activities.

484 **4. CONCLUSIONS**

485 PM_1 samples have been collected at an urban background site in Venice (Po Valley, Italy), within
486 one of the most polluted areas in Europe. The main components of PM were determined: water
487 soluble inorganic ions, elements, elemental and organic carbon. Collected data have been processed
488 to (i) determine seasonal behaviour, (ii) estimate secondary inorganic and organic aerosol, (iii)
489 estimate major components applying a mass closure model and (iv) identify and quantify most

490 probable sources by using positive matrix factorization (PMF) and hypothesize their location by
491 using CPF. Therefore, the main findings can be summarized as follows:

492 • During the winter PM_1 fraction makes the highest contribution to PM_1 reaching about 60%
493 of mass.

494 • Total carbon (TC) and secondary inorganic aerosol (SIA) represent the main components of
495 PM_1 reaching 34% and 22% of the annual mean, respectively. During winter these
496 components make up about 68% of PM; on the contrary during summer the elemental
497 contribution increases and reaches 24%.

498 • Ammonium, nitrate and sulphate contribute about 76 % of the total inorganic ionic species
499 mass (83% and 69% in winter and summer period, respectively).

500 • On an annual basis nitrate, sulphate, potassium and calcium represent the main inorganic
501 component of PM_1. Among the analysed elements only Ti, Ba, Ni, Cd and Sb do not show a
502 statistically significant seasonal difference. The others present a marked seasonal difference,
503 with the highest concentration in winter, except for Ni and V. This indicates that different
504 processes and sources are involved in PM_1 formation and emission and these are strongly
505 influenced by weather conditions.

506 • Over the whole period OC ranged from 0.4 to 45.0 µg m^{-3} and EC ranged from 0.1 to 9.6 µg
507 m^{-3}. Despite the OC/EC ratio presenting higher values during winter than in summer (3.1
508 and 1.6 µg m^{-3} mean, respectively) indicating a greater contribution of secondary aerosol
509 during the winter, the percentage contribution of SOC to total OC is higher in summer
510 (54%) than in winter (39.5%). This is in agreement with enhanced photochemical formation
511 due to the increase of solar radiation during summer, and exceeds the influence of lower
512 temperatures upon partitioning of semi-volatiles.

513 • During winter OM and secondary components dominate the PM mass. On the contrary, in
514 summer the major contributor to PM is mineral dust and increased marine components

(NaCl). When highly polluted events occur (PM_1 > 50 µg m^{-3}, 17 days) no significant differences can be observed in PM_1 composition. Therefore, the increase in PM_1 concentration appears to be due to a simultaneous increase of all components.

- Seven PM_1 sources have been identified, among these biomass burning (33%) and secondary inorganic aerosol (33%) are the major contributors in winter, while in summer the aged sulphate contribution increases (22%) as well as fossil fuels (14%) and marine aerosol (10%) due to the decrease of the typical winter sources.

Although PM_1 is not regulated at European level, it could represent a better indicator of anthropogenic PM sources; in winter it represents the greatest part of PM_{10} and $PM_{2.5}$.

ACKNOWLEDGMENTS

The authors would to thank Prof. E. Argese, L. Gobbo for the analytical support. Ente della Zona Industriale di Porto Marghera supplied weather data.

DISCLAIMER

The views expressed in this study are exclusively of the authors and may not reflect those of ARPAV.

REFERENCES

Anderson, J. O., Thundyil, J. G., Stolbach, A., 2012. Clearing the Air: A Review of the Effects of Particulate Matter Air Pollution on Human Health. J. Med. Toxicol. 8,166 – 175.

Birch, M. E. and Cary, R. A., 1996. Elemental Carbon-Based Method for Monitoring Occupational Exposures to Particulate Diesel Exhaust. Aerosol Sci. Tech. 25, 221–241.

Birmili, W., Allen, A. G., Bary, F., Harrison, R. M., 2006. Trace Metal Concentrations and Water Solubility in Size-Fractionated Atmospheric Particles and Influence of Road Traffic. Environ. Sci. Technol. 40, 1144-1153.

Bougiatiati, A., Zarmpas, P., Koulouri, E., Antoniou, M., Theodosi, C., Kouvarakis, G., Saarikoski, S., Mäkelä, T., Hillamo, R., Mihalopoulos, N., 2013. Organic, elemental and water-soluble organic carbon in size segregated aerosols, in the marine boundary layer of the Eastern Mediterranean. Atmos. Environ. 64, 251–262.

Cabada, J. C., Pandis, S. N., Subramanian, R., Robinson, A. L., Polidori, A., Turpin, B., 2004. Estimating the Secondary Organic Aerosol Contribution to PM 2.5 Using the EC Tracer Method Special Issue of Aerosol Science and Technology on Findings from the Fine Particulate Matter Supersites Program. Aerosol Sci. Tech. 38:S1, 140–155.

Castro, L.M., Pio, C.A., Harrison, R.M., Smith, D.J.T., 1999. Carbonaceous aerosol in urban and rural European Atmospheres: Estimation of secondary organic carbon concentrations. Atmos. Environ. 33, 2771-2781.

Cheng, Y., Zou, S. C., Lee, S .C., Chow, J. C., Ho, K. F., Watson, J. G., Han, Y. M., Zhang, R. J., Zhang, F., Yau, P. S., Huang, Y., Bai, Y., Wu, W. J., 2011. Characteristics and source apportionment of PM1 emissions at a roadside station. J. Hazard. Mater. 195, 82–91.

Chow, J. C., Lowenthal, D. H., Chen, L.-W. A., Wang, X., Watson, J., G., 2015. Mass reconstruction methods for PM2.5: a review. Air Qual. Atmos. Health 8, 243–263.

Donahue, N.M., Robinson, A.L., Stanier, C.O., Pandis, S.N., 2006. Coupled partitioning, dilution and chemical aging of semivolatile organics. Environ. Sci. Technol. 40, 2635–2643.

Fernandez Espinosa, A. J., Ternero Rodrígues, M., Barragán de la Rosa, F. J., Jiménez Sánchez, J. C., 2001. Size distribution of metals in urban aerosols in Seville (Spain). Atmos. Environ. 35, 2595–2601.

Harrison, R. M., Jones, A. M., Lawrence, R. G., 2003. A pragmatic mass closure model for airborne particulate matter at urban background and roadside sites. Atmos. Environ. 37, 4927–4933.

Harrison, R. M., Yin, J., 2008. Sources and processes affecting carbonaceous aerosol in central England. Atmos. Environ. 42, 1413–1423.

ISPRA, 2015. Italian Institute for Environmental Protection and Research. Disaggregated emission inventory. Available online: http://www.sinanet.isprambiente.it/it/inventaria/ disaggregazione-dellinventario-nazionale-2010, last access: 30 April 2015

584 ISTAT, 2011. Italian Institute of Statistics. Data warehouse of the 2011 Population and housing
585 census. Available on-line:http://dati-censimentopopolazione.istat.it/#
586
587 Karthykeyan, S., Joschi, U. M., Balasubramanian, R., 2006. Microwave assisted sample preparation
588 for determining water-soluble fraction of trace elements in urban particulate matter: Evaluation of
589 bioavailability. Anal. Chim. Acta 576, 23–30.
590
591 Kim, E., Hopke, P.K., Edgerton, E.S., 2003. Source Identification of Atlanta Aerosol by Positive
592 Matrix Factorization. J. Air Waste Manage. Assoc. 53, 731–739.
593
594 Kim, E., Hopke, P.K., Kenski, D.M., Koerber, M., 2005. Sources of Fine Particles in a Rural
595 Midwestern U.S. Area. Environ. Sci. Technol. 39, 4953–4960.
596
597 Larsen, B. R., Gilardoni, S., Stenström, K., Niedzialek, J., Jimenez, J., Belis, C.A., 2012. Sources
598 for PM air pollution in the Po Plain, Italy: II. Probabilistic uncertainty characterization and
599 sensitivity analysis of secondary and primary sources. Atmos. Environ. 50, 203–213.
600
601 Marcazzan, G.M., Vaccaro, S., Valli, G., Vecchi R., 2001. Characterisation of PM10 and PM2.5
602 particulate matter in the ambient air of Milan (Italy). Atmos. Environ. 35, 4639–4650.
603
604 Masiol, M., Agostinelli, C., Formenton, G., Tarabotti, E., Pavoni, B., 2014a. Thirteen years of air
605 pollution hourly monitoring in a large city: Potential sources, trends, cycles and effects of car-free
606 days. Sci. Total Environ. 494–495, 84–96.
607
608 Masiol, M., Squizzato, S., Rampazzo, G., Pavoni, B., 2014b. Source apportionment of $PM_{2.5}$ at
609 multiple sites in Venice (Italy): Spatial variability and the role of weather. Atmos. Environ. 98, 78–
610 88.
611
612 Masiol M., Benetello F., Harrison R.M., Formenton G., De Gaspari F., Pavoni B., 2015a. Spatial,
613 seasonal trends and transboundary transport of $PM_{2.5}$ inorganic ions in the Veneto Region
614 (Northeast Italy). Atmos. Environ.117, 19–31.
615
616 Masiol, M., Squizzato, S., Ceccato, D., Pavoni, B., 2015b. The size distribution of chemical
617 elements of atmospheric aerosol at a semi-rural coastal site in Venice (Italy). The role of
618 atmospheric circulation. Chemosphere 119, 400–406.
619
620 McDonald, J. D., Zielinska, B., Fujita, E. M., Sagebiel, J. C., Chow, J. C., Watson, J. G., 2000.
621 Fine Particle and Gaseous Emission Rates from Residential Wood Combustion. Environ. Sci.
622 Technol. 34, 2080–2091.
623
624 Moreno, T., Alastuey, A., Querol, X., Font, O., Gibbons, W., 2007. The identification of metallic
625 elements in airborne particulate matter derived from fossil fuels at Puertollano, Spain. Int. J. Coal
626 Geol. 71, 122 – 128.
627
628 Pant, P., Harrison, R.M., 2013. Estimation of the contribution of road traffic emissions to
629 particulate matter concentrations from field measurements: A review. Atmos. Environ.77, 78–97.
630
631 Pérez, N., Pey, J., Querol, X., Alastuey, A., López, J., Viana, M., 2008. Partitioning of major and
632 trace components in PM_{10}–$PM_{2,5}$–PM_1 at an urban site in Southern Europe. Atmos. Environ. 42(8),
633 1677–1691.
634

635 Perrone, M.R., Becagli, S., J.A. Garzia Orza, Vecchi, R., Dinoi, A., Udisti, R., Cabello, M., 2013.
636 The impact of long-range-transport on PM_1 and $PM_{2.5}$ at a Central Mediterranean site. Atmos.
637 Environ. 7, 176–186.
638
639 Pio, C.A., Legrand, M., Oliveira, T., Afonso, J., Santos, C., Caseiro, A., Fialho, P., Barata, F.,
640 Puxbaum, H., Sanchez-Ochoa, A., Kasper-Giebl, A., Gelencsér, A., Preunkert, S., Schock, M.,
641 2007. Climatology of aerosol composition (organic versus inorganic) at nonurban sites on a west-
642 east transect across Europe. J. Geophys. Res 112, D23S02.
643
644 Polissar, A.V., Hopke, P.K., Paatero, P., Malm, W.C., Sisler, J.F., 1998. Atmospheric aerosol over
645 Alaska 2. Elemental composition and sources. J. Geophys. Res. 103 (D15), 19045-19057.
646
647 Pope III, C.A., Dockery, D.W., 2006. Health effects of fine particulate air pollution: lines that
648 connect. J. Air Waste Manage. 56, 709–42.
649
650 Querol, X., Viana, M., Alastuey, A., Amato, F., Moreno, T., Castillo, S., Pey, J., et al., 2007. Source
651 origin of trace elements in PM from regional background, urban and industrial sites of Spain.
652 Atmos. Environ. 41, 7219 – 7231.
653
654 Reche, C., Viana, M., Amato, F., Alastuey, A., Moreno, T., Hillamo, R., Teinilä, K., Saarnio, K.,
655 Seco, R., Peñuelas, J., Mohr, C., Prévôt, A.S.H., Querol, X., 2012. Biomass burning contributions
656 to urban aerosols in a coastal Mediterranean City. Sci. Total Environ. 427–428, 175–190.
657
658 Reff, A., Eberly, S.I., Bhave, P.V., 2007. Receptor modeling of ambient particulate matter data
659 using positive matrix factorization: review of existing methods. J. Air Waste Manage. 57, 146–154.
660
661 Rohr, A. C., Wyzga, R. E., 2012. Attributing health effects to individual particulate matter
662 constituents. Atmos. Environ. 62, 130–152.
663
664 Samara, C., Voutsa, D., 2005. Size distribution of airborne particulate matter and associated heavy
665 metals in the roadside environment. Chemosphere 59, 1197–1206.
666
667 Schaap, M., Spindler, G., Schulz, M., Acker, K., Maenhaut, W., Berner, A., Wieprecht, W., Streit,
668 N., Müller, K., Brüggemann, E., Chi, X., Putaud, J. P., Hitzenberger, R., Puxbaum, H.,
669 Baltensperger, U., and ten Brink, H., 2004. Artefacts in the sampling of nitrate studied in the
670 "INTERCOMP" campaigns of EUROTRAC-AEROSOL. Atmos. Environ. 38, 6487–6496.
671
672 Seinfeld, J. H. and Pandis, S. N., 2006. Atmospheric Chemistry and Physics: From Air Pollution To
673 Climate Change, 2nd ed., John Wiley & Sons, New York.
674
675 Squizzato, S., Masiol, M., Innocente, E., Pecorari, E., Rampazzo, G., Pavoni, B., 2012. A procedure
676 to assess local and long-range transport contributions to PM2.5 and secondary inorganic aerosol. J.
677 Aerosol Sci. 46, 64–76.
678
679 Squizzato, S., Masiol, M., Brunelli, A., Pistollato, S., Tarabotti, E., Rampazzo, G., Pavoni, B.,
680 2013. Factors determining the formation of secondary inorganic aerosol: a case study in the Po
681 Valley (Italy). Atmos. Chem. Phys. 13(4), 1927–1939.
682
683 Theodosi, C., Grivas, G., Zarmpas, P., Chaloulakou, A., Mihalopoulos, N., 2011. Mass and
684 chemical composition of size-segregated aerosols (PM_1, $PM_{2.5}$, PM_{10}) over Athens, Greece: local
685 versus regional sources. Atmos. Chem. Phys. 11, 11895–11911.

Turpin, B.J., Huntzicker, J.J., 1991. Secondary formation of organic aerosol in the Los Angeles basin: A descriptive analysis of organic and elemental carbon concentrations. Atmos. Environ. Part A. General Topics 25, 207–215.

Turpin, B. J., Huntzinker, J. J., 1995. Identification of secondary organic aerosol episodes and quantification of primary and secondary inorganic aerosol concentrations during SCAQS. Atmos. Environ. 29, 3527–3544.

USEPA (United States Environmental Protection Agency), 2014. EPA positive matrix factorization (PMF) 5.0. In: Fundamentals & User Guide. USEPA Office of Research and Development, Washington DC, USA, 124 pp.

Valotto, G., Squizzato, S., Masiol, M., Zannoni, D., Visin, F., Rampazzo, G., 2014. Elemental characterization, sources and wind dependence of PM_1 near Venice, Italy. Atmos. Res.143, 371–379.

Vecchi, R., Marcazzan, G., Valli, G., Ceriani, M., Antoniazzi, C., 2004. The role of atmospheric dispersion in the seasonal variation of PM_1 and $PM_{2,5}$ concentration and composition in the urban area of Milan (Italy). Atmos. Environ. 38, 4437–4446.

Vecchi, R., Chiari, M., D'Alessandro, A., Fermo, P., Lucarelli, F., Mazzei, F., Nava, S., Piazzalunga, A., Prati, P., Silvani, F., et al. 2008. A mass closure and PMF source apportionment study on the sub-micron sized aerosol fraction at urban sites in Italy. Atmos. Environ. 42, 2240–2253.

Yin, J., Harrison, R. M., 2008. Pragmatic mass closure study for $PM_{1.0}$, $PM_{2.5}$ and PM_{10} at roadside, urban background and rural sites. Atmos. Environ. 42, 980–988.

Figure 1. Study area and sampling site location (images from Google Earth).

Figure 2. Comparison between calculated and measured ammonium in PM_1 (ammonium sulphate: calculated $NH_4^+ = 0.38* [SO_4^{2-}] + 0.29 *[NO_3^-]$; ammonium bisulphate: calculated $NH_4^+ = 0.192* [SO_4^{2-}] + 0.29 *[NO_3^-]$).

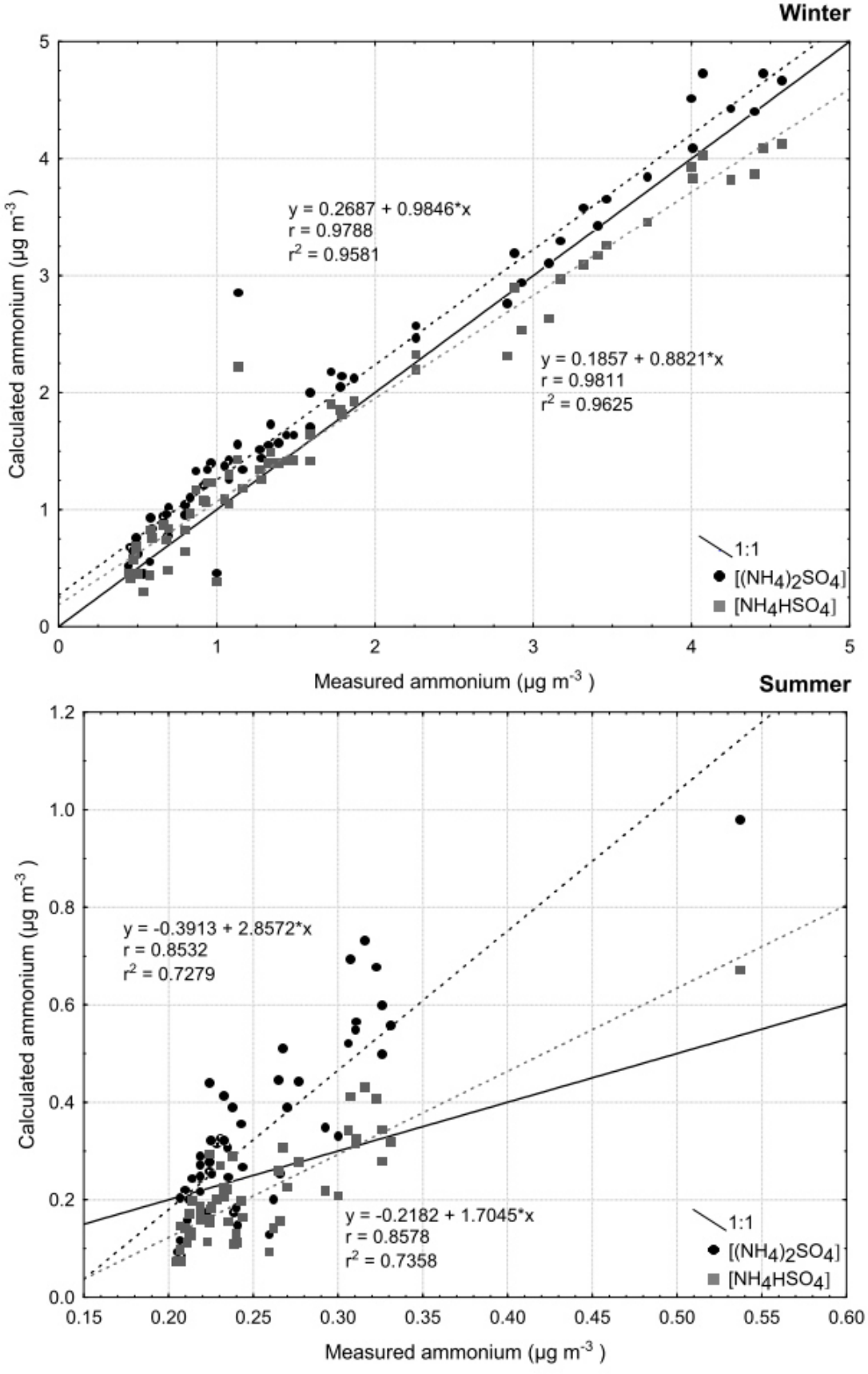

Figure 3. Comparison of mean composition of PM1 in winter, summer and during high pollution events (PM_1 > 50 µg m^{-3}).

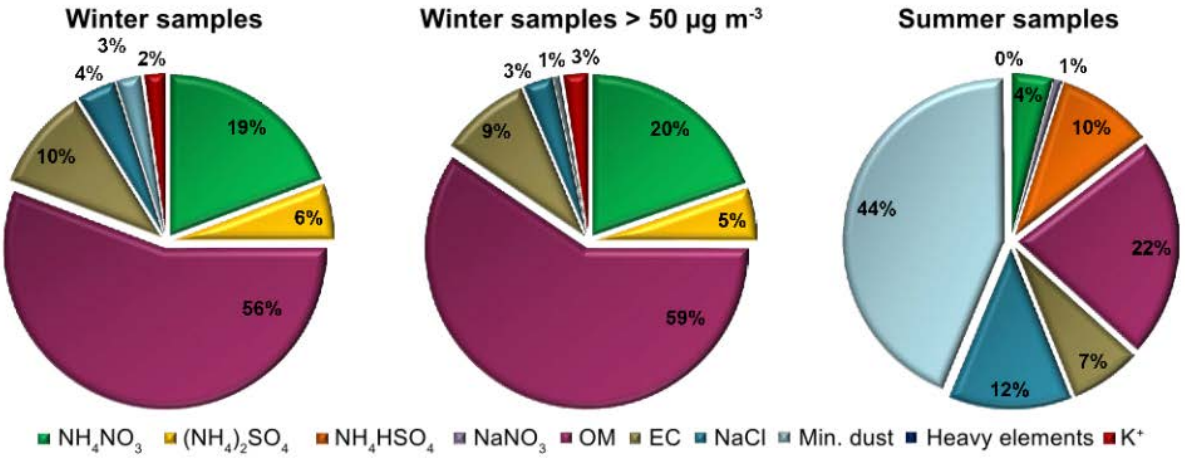

Figure 4. Factor profiles obtained by PMF analysis.

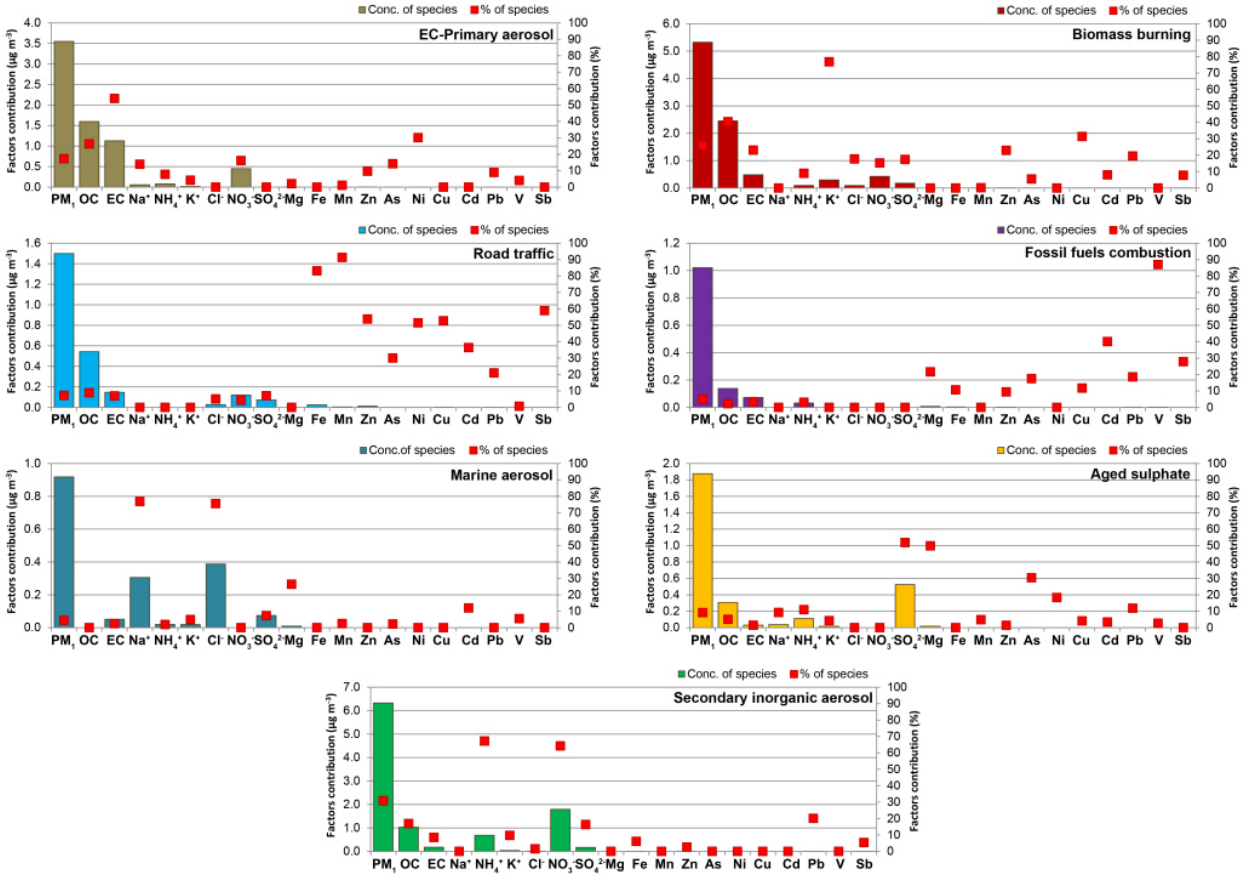

Figure 5. CPF plots for the highest 25% of the mass contributions.

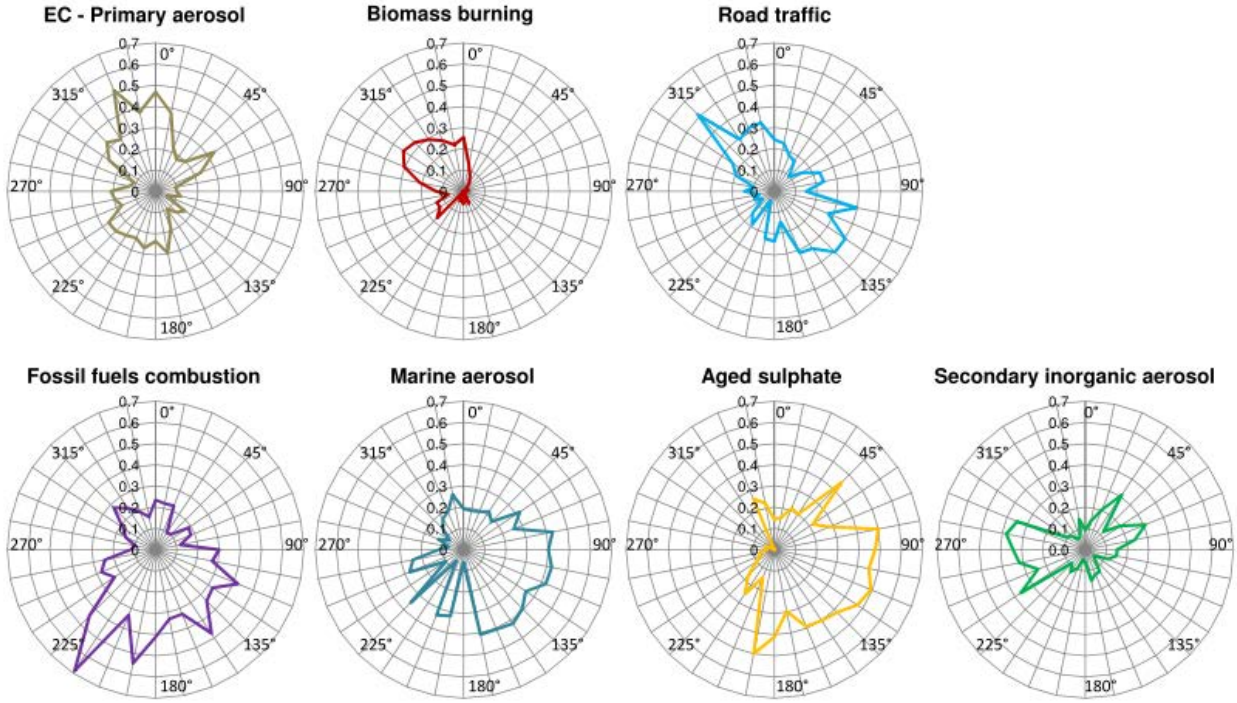

763 **Table 1.** Basic statistics of experimental values of PM_1, PM_{10}, organic and elemental carbon,
764 inorganic ions, elements, gaseous pollutants and meteorological conditions for each season and
765 whole sampling period. Analytical data refer to PM_1 fraction of particles.
766

		All		Winter[a]		Summer[b]	
		Valid N	Mean ± S.D.	Valid N	Mean ± S.D.	Valid N	Mean ± S.D.
PM_1	µg m^{-3}	117	21±22	61	34±24	56	6.4±2
PM_{10}	µg m^{-3}	117	37±32	61	57±33	56	16±7
PM_1/PM_{10}	µg m^{-3}	117	0.5±0.2	61	0.6±0.1	56	0.4±0.1
OC	µg m^{-3}	117	7±9	61	11.6±10	56	1.1±1
EC	µg m^{-3}	117	2.1±2.2	61	3.5±2.2	56	0.6±1
OC/EC		117	2.5±1	61	3.1±1	56	1.6±1
TC	%	117	34±14	61	42.5±11.5	56	25±10
Na^+	µg m^{-3}	85	0.5±0.3	37	0.7±0.3	48	0.4±0.3
NH_4^+	µg m^{-3}	115	1±1.2	60	1.8±1	55	0.3±0.1
K^+	µg m^{-3}	75	0.6±0.7	58	0.8±1	17	0.1±0.1
Mg^{++}	µg m^{-3}	40	0.1±0.1	33	0.1±0	7	0.1±0.1
Cl^-	µg m^{-3}	79	0.7±0.5	48	0.8±1	31	0.6±0.4
NO_3^-	µg m^{-3}	117	2.8±3.4	61	5±3	56	0.3±0.2
SO_4^{2-}	µg m^{-3}	116	1±0.8	61	1.4±1	55	0.6±0.4
SIA[c]	%	117	22±7	61	25.3±7	56	18±4
Ca	ng m^{-3}	74	669±366	30	421±203	44	839±357
Mg	ng m^{-3}	78	384±262	37	176±140	41	572±196
Al	ng m^{-3}	79	327±243	32	124±62	47	465±222
Fe	ng m^{-3}	49	81±103	30	101±114	19	51±76
K	ng m^{-3}	111	457±611	59	772±699	52	99±59
S	ng m^{-3}	110	487±336	57	603±396	53	362±192
Ti	ng m^{-3}	95	2.4±1.2	48	2.2±1	47	2.5±1
Mn	ng m^{-3}	113	5±12	57	8.8±16	56	1.9±1
Zn	ng m^{-3}	101	28±30	60	39.6±34	41	10.7±7
Ba	ng m^{-3}	39	10±30	4	53±90.9	35	4.7±3
As	ng m^{-3}	110	1.2±1.3	59	1.5±2	51	0.8±1
Ni	ng m^{-3}	67	2.5±1.9	42	1.9±2	25	3.5±1
Cu	ng m^{-3}	89	8±25	53	12.7±32	36	1.6±1
Cd	ng m^{-3}	100	1.1±1.1	51	1.2±1	49	1.1±1
Pb	ng m^{-3}	116	7±7	60	10.5±8	56	3.2±2
V	ng m^{-3}	107	2.4±2.1	53	1.9±2	54	2.8±2
Sb	ng m^{-3}	95	1.6±2.1	44	2.5±3	51	0.9±1
Σelements[d]	%	117	13±17	61	2.5±3	56	24±18
Total accounted	%	117	76±15	61	75±9	56	76±20
CO	mg m^{-3}	117	0.7±0.5	61	1.0±0.5	56	0.3±0.1
NO	µg m^{-3}	117	37±53	61	68±59	56	4±4
NO_2	µg m^{-3}	117	34±12	61	40±12	56	26±6

NO_x	µg m^{-3}	117	90±92	61	143±100	56	32±10
SO_2	µg m^{-3}	117	1.6±1.1	61	1.4±0.9	56	1.7±1
Solar radiation[e]	W m^{-2}	117	3270±2702	61	828±461	56	5930±1159
Temperature	°C	117	15±7	61	8±2	56	22±3
Relative humidity	%	117	82±13	61	93±6	56	71±9
Wind speed	m s^{-1}	117	2.1±1	61	1.7±1	56	2.6±1
Rain[f]	mm	117	345	61	248	56	98

Note:
[a]Winter: December 7, 2013 –February 5, 2014.
[b]Summer: May 7, 2014 – July 1, 2014.
[c]SIA (secondary inorganic aerosol) is expressed as sum of NH_4^+, NO_3^- and SO_4^{2-}.
[d]Σelements represents the sum of all elements except K and S which are included as K^+ and SO_4^{2-}.
[e]Solar radiation is presented as the mean of the daily total radiation during the reporting period.
[f]Rain is presented as the total precipitation during the reporting period.

Table 2. Comparison with previous studies available in the literature for similar sampling sites. PM, OC, EC and ions are in μg m^{-3}, elements in ng m^{-3}.

	This study			Valotto et al., 2014		Squizzato et al., 2013; Masiol et al., 2014b		Perez et al., 2008	Vecchi et al., 2004		Vecchi et al., 2008						Harrison and Yin, 2008	
	Via Lissa (UB)			Marco Polo Airport (Venice)		Via Lissa (UB)		Barcelona (UB+traffic)	Milano (UB+traffic)		Milano (UB)		Firenze (UB)		Genova (UB)		Birmingham (UB)	
	Winter	Summer	Mean	Winter	Summer	Winter	Summer	Mean	Winter	Summer	Winter	Summer	Winter	Summer	Winter	Summer	Winter	Summer
PM_{10}	56.9	16.3	37.5	45.2	19.3													
$PM_{2.5}$						51.0	15.0											
PM1	34.3	6.4	20.9	26.6	5.8			19	41.0	16.4	48.8	19.4	25.3	11.8	11.5	17.4	12.6	9.2
PM_1/PM_{10}	0.6	0.4	0.5	0.6	0.3													
OC	11.8	1.1	6.7					4.3	17.8	6.1	14.80	4.80	12.00	2.70	5.00	3.40	2.8	2
EC	3.5	0.6	2.1					1.8	2.3	1.3	1.80	1.10	0.90	0.60	0.90	0.90	1.8	0.9
OC/EC	3.4	1.9	2.7					2.4	7.6	4.7	8.2	4.4	13.3	4.5	5.6	3.8		
NO_3^-	5.0	0.3	2.8			6.1	0.5	1.5			13.6	0.9	3.2	0.1	1.1	0.2	1.8	0.4
SO_4^{2-}	1.4	0.6	1.0			3.8	2.7	3.3			4.7	3.9	1.7	3.2	1.7	3.8	1.3	2.0
NH_4^+	1.8	0.3	1.0			3.3	1.0	1.2			4.2	1.8	1.6	1.3	1	1.4		
SIA	8.0	1.2	4.6			13.1	4.0	6			22.5	6.6	6.5	4.6	3.8	5.4		
Ti	2.2	2.5	2.4	2.7	9.9	5.7	15.4	1.8	7	4	4	4	4	4	4	4		
Mn	8.8	1.9	5.4	2.8	0.9	11.3	3.8	4	9	4	9	5	2	2	1	3		
Zn	39.6	10.7	27.9	22.1	3.4	50.8	20.1	48	66	32	59	34	20	9	13	9		
Cu	12.7	1.6	8.2	3	0.5	18.7	6.1	12	7	3	7	4	4	4	2	7		
Ba	53.0	4.7	9.6	1.3	9.9	17.8	5.3	9										
Fe	100.7	51.1	81.4	36.8	11.2	255.0	164.0				86	42	41	26	24	37	100	20
K	771.9	98.8	456.6	528.5	31.4	967.0	134.0		257	81	300	98	270	94	91	59		
Ca	420.6	838.8	669.3	60	297.3	211.0	354.0		24	17	27	22	28	34	18	56	40	50
Mg	176.2	572.1	384.3	34.7	37.5	115.0	73.0											
Al	124.4	465.1	327.1	19.6	9.3	97.0	220.0		16	14	16	11	12	19	14	16		
S	602.7	362.2	486.8	586.6	523.3	1267.0	1340.0		1297	1445	1200	1500	560	1100	550	1000		
V	1.9	2.8	2.4	8	8.5	2.4	5.4	6	5	4	4	4	3	4	4	15		
Ni	1.9	3.5	2.5	1.7	0.6	2.3	4.7	3	7	2								
Pb	10.5	3.2	7.0			18.5	7.7	17	35	15								
As	1.5	0.8	1.2			2.1	1.7	0.6	2	1								
Cd	1.2	1.1	1.1	0.7	0.3	1.3	1.3	0.3										

UB: urban background site.

779 **Table 3.** Estimate of primary and secondary organic carbon (average concentrations) during winter and summer period and relationship with K^+,
780 NO_3^- and SO_4^{2}.
781
782

EC-tracer method		[OC/EC]p	Non-combustion primary OC, *b* ($\mu g\ m^{-3}$)	R^2	SOC $\mu g\ m^{-3}$	POC $\mu g\ m^{-3}$	POC vs K^+	SOC vs NO_3^-	SOC vs SO_4^{2-}
Cabada et al. (2004)	Winter	1.87	0.173	0.92	5.4 (37%)	6.7	r=0.77	r=0.73	r=0.75
	Summer	1.49	-0.0161	0.81	0.6 (55%)	0.9	r=0.58	r=-0.23	r=-0.14
Harrison and Yin (2008)	Winter	1.78		0.99	5.8 (42%)	6.2	r=0.77	r=0.74	r=0.76
	Summer	1.04		0.93	0.6 (53%)	0.6	r=0.57	r=0.04	r=0.31

783

784 **Table 4.** Conversion factors used in mass closure and regression results (*y*, mass reconstructed using mass closure model and *x*, gravimetrically
785 measured mass).
786

Season	Secondary inorganic ions	Organic mass	Elemental carbon	Geological minerals/road dust	Salt	Trace elements	Others	Regression
Winter (n = 61)	1.375 SO_4^{2-} as $(NH_4)_2SO_4$[a] 1.29 NO_3^- as NH_4NO_3[a]	1.6 OC[b]	1 EC[a]	1.89Al+2.14Si+1.4Ca+ 1.43Fe*+1.67Ti+1.2K*[c,d]	1.65Cl^- as NaCl[a]	1.25 Cu + 1.24 Zn + 1.08 Pb[c]	K^+	$y = 0.96x + 0.17$
Summer (n = 56)	1.29 SO_4^{2-} as NH_4HSO_4[a] 1.29*(0.85 NO_3^-) as NH_4NO_3[a] 1.37*(0.15 NO_3^-) as $NaNO_3$[a]	1.6 OC[b]	1 EC[a]	1.89Al+2.14Si+1.4Ca+ 1.43Fe*+1.67Ti+1.2K*[c,d]	1.65Cl^- as NaCl[a]	1.25 Cu + 1.24 Zn + 1.08 Pb[c]	K^+	$y = 1.39x - 1.27$

787 [a] Harrison et al., 2003.
788 [b] Marcazzan et al., 2001.
789 [c] Chow et al., 2015 and references therein.
790 [d] Si concentration has been obtained from the Al/Si ratio (0.46); Fe* and K* indicate the part of iron and potassium concentration considered of crustal origin. As the first
791 approximation: for Fe this fraction has been evaluated dividing the total concentration of this element for its $EF_{Al;}$ for K this fraction has been calculated subtracting the K^+ to K
792 total considering K^+ as a marker of biomass combustion.
793
794
795